Archival Report

Biological Psychiatry

The Genetic Architecture of Amygdala Nuclei

Mary S. Mufford, Dennis van der Meer, Tobias Kaufmann, Oleksandr Frei, Raj Ramesar, Paul M. Thompson, Neda Jahanshad, Rajendra A. Morey, Ole A. Andreassen, Dan J. Stein, and Shareefa Dalvie

ABSTRACT

BACKGROUND: Whereas genetic variants influencing total amygdala volume have been identified, the genetic architecture of its distinct nuclei has yet to be explored. We aimed to investigate whether increased phenotypic specificity through nuclei segmentation aids genetic discoverability and elucidates the extent of shared genetic architecture and biological pathways with related disorders.

METHODS: T1-weighted brain magnetic resonance imaging scans (N = 36,352, 52% female) from the UK Biobank were segmented into 9 amygdala nuclei with FreeSurfer (version 6.1). Genome-wide association analyses were performed on the entire sample, a European-only subset (n = 31,690), and a generalization (transancestry) subset (n = 4662). We estimated single nucleotide polymorphism–based heritability; derived polygenicity, discoverability, and power estimates; and investigated genetic correlations and shared loci with psychiatric disorders.

RESULTS: The heritability of the nuclei ranged from 0.17 to 0.33. Across the whole amygdala and the nuclei volumes, we identified 28 novel genome-wide significant ($p_{adj} < 5 \times 10^{-9}$) loci in the European analysis, with significant en masse replication for the whole amygdala and central nucleus volumes in the generalization analysis, and we identified 10 additional candidate loci in the combined analysis. The central nucleus had the highest statistical power for discovery. The significantly associated genes and pathways showed unique and shared effects across the nuclei, including immune-related pathways. Shared variants were identified between specific nuclei and autism spectrum disorder, Alzheimer's disease, Parkinson's disease, bipolar disorder, and schizophrenia.

CONCLUSIONS: Through investigation of amygdala nuclei volumes, we have identified novel candidate loci in the neurobiology of amygdala volume. These nuclei volumes have unique associations with biological pathways and genetic overlap with psychiatric disorders.

https://doi.org/10.1016/j.biopsych.2023.06.022

The amygdala is a subcortical brain region involved in emotional processing, social cognition, memory, and decision making (1,2). The twin-based heritability of amygdala volume is approximately 43% (3), with single nucleotide polymorphism (SNP)–based heritability ranging from 9% to 17% (4). To date, only 1 locus on chromosome 12, rs17178006, has been significantly associated with amygdala volume (4). However, the genetic architecture of amygdala nuclei volumes has yet to be explored. Mapping this architecture will contribute to a deeper understanding of amygdala neurobiology and inform the future discovery of treatments that target the amygdala.

Both human and animal models have identified 3 broad subdivisions of the amygdala, the basolateral, centromedial, and cortical-like complexes, which can be further divided into 9 distinct nuclei (5). These complexes have different functional connectivity and roles in threat processing (5). The basolateral amygdala consists of lateral, basal, accessory, and paralaminar nuclei. These nuclei evaluate sensory information and integrate with cortical association areas that regulate cognitive processing, fear, and other emotional responses (6). The centromedial amygdala consists of the central and medial nuclei and is critical for orchestrating fear responses, such as increased cardiovascular output, via connections with the hypothalamus, basal forebrain, and brainstem (5). The cortical-like nuclei include the cortical nucleus and corticoamygdaloid transition area, which have roles in olfactory fear conditioning (7) and social communication (8), respectively. Nuclei including the anterior amygdaloid area, about which very little is known, do not fit into the 3 broad subdivisions of the amygdala. The distinct nuclei have individual roles that contribute to the broader functions of each subdivision. The recent development of an automated segmentation algorithm to extract the 9 nuclei (9) provided us with the opportunity to investigate each of the nuclei.

Reduced amygdala volume has been reported in several disorders, e.g., schizophrenia (10), bipolar disorder (11), posttraumatic stress disorder (12,13), and Alzheimer's disease (14). Case-control comparisons of schizophrenia and bipolar disorder have demonstrated volume reductions for all nuclei except the medial and central nuclei (15). Reduced volumes in patients may be partly genetic in origin, making investigations into the shared genetic architecture between

ISSN: 0006-3223

brain volumes and disorders a valuable area of research for the clinical neurosciences (16–18). Studies investigating the genetics of subregional volumes of other brain regions, e.g., the hippocampus, thalamus, and brainstem, have highlighted the power of this approach (16–18).

Investigating the genetic architecture of amygdala nuclei is needed to provide insights into their unique and shared genetic architecture and underlying biological pathways. An improved understanding of amygdala neurobiology will help illuminate the pathophysiology of associated disorders. We segmented the amygdala into its 9 constituent nuclei with the aim of studying the genetic underpinnings of amygdala nuclei volumes and their associations with relevant disorders. Our goals were supported by analyzing SNP-based heritability and genetic correlations and by assessing loci that influence multiple nuclei.

METHODS AND MATERIALS

Participants

Individual-level genotype and structural brain magnetic resonance imaging data were sourced from the UK Biobank (UKB) (n = 42,067) (19,20) under accession code 27412. Each sample was collected with participants' written informed consent for study procedures approved by local institutional review boards. Of these participants, 3742 (8.9% of the total) had an ICD-10 code corresponding to a neurological or mental disorder (code F or G). These individuals were excluded from our analyses (Table T1 in Supplement 2) to maintain a cohort of healthy individuals. The cohort we analyzed contained 36,352 participants with an age range of 44 to 82 years (mean age = 64.26, SD = 7.5), and 52% of the participants were female. The primary dataset contained 31,690 participants, and the generalization dataset contained 4662 participants.

Magnetic Resonance Imaging Data Processing

T1-weighted magnetic resonance imaging volumes were processed using the FreeSurfer recon-all stream (version 5.3; http://surfer.nmr.mgh.harvard.edu). The amygdala was segmented into 9 nuclei (anterior amygdaloid area; cortico-amygdaloid transition area; and basal, lateral, accessory basal, central, cortical, medial, and paralaminar nuclei) (Figure 1) using FreeSurfer (version 6.1) (9). We used this automated segmentation because the current gold standard for manual segmentation is impractical for use with such large datasets. Given that the spatial reliability of the segmentation varies according to the size of each nucleus (21), we performed binomial tests to investigate the correlations between our results for nucleus volume, heritability, and the number of significant loci (see Supplementary note 1 in Supplement 1). Furthermore, individual nuclei volumes ±4 SDs from the mean of the Euler number, the mean on any amygdala measure, or the intracranial volume were excluded from further analyses (22) (Table T1 in Supplement 2). The nuclei volumes were found to be normally distributed (Figure S1 in Supplement 1; Table T2 in Supplement 2).

Genotyping and Quality Control

Phased and imputed genome-wide genetic data were obtained from the UKB (version 3) (20). Participants in the primary analysis were restricted to individuals of European ancestry as determined through self-report and validated with principal component analysis by the UKB (23). Individuals of non-European ancestry were grouped together in the generalization analysis including self-reported European participants who did not meet principal component analysis requirements and participants of African, South Asian, East Asian, mixed, and other ancestries (Table T5 in Supplement 2). The primary and generalization analyses were also grouped together in a combined analysis. Postimputation quality checks, performed using PLINK (version 1.9) (24), included the removal of poorly imputed SNPs (estimated $R^2 < 0.5$), SNPs with low minor allele frequency (<0.1%), and SNPs that were not in Hardy-Weinberg equilibrium ($p < 1 \times 10^{-9}$) (Table T1 in Supplement 2).

Statistical Analyses

Because volumetric and genetic correlations between right and left brain hemispheres were relatively high for most structures (Table T3 in Supplement 2), we summed the estimates of both hemispheres to reduce the number of analyses and the burden of multiple testing correction. Generalized additive model fitting in R (version 3.5) was used on the total sample to regress out the effects of the covariates from each outcome measure. The covariates were scanner, sex, age, age^2, the first 10 principal components to account for population stratification and genotyping artifacts, intracranial volume, and whole amygdala volume. Whole amygdala volume was included as a covariate to isolate the contribution from the unique genetic

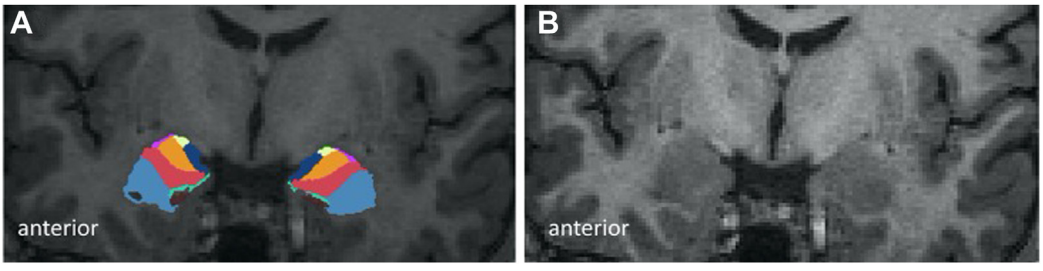

Figure 1. Segmentation of the amygdala nuclei. **(A)** Using FreeSurfer (version 6.1), the amygdala was segmented into 9 nuclei: anterior amygdaloid area = yellow, cortico-amygdaloid transition area = dark blue, basal = red, lateral = light blue, accessory basal = orange, central = purple, medial = green. The cortical and paralaminar nuclei are not shown here. **(B)** Structural T1 scan provided for reference. Images provided by Morey *et al.* (12).

architecture of each nucleus. The results without this correction for the whole amygdala volume are shown in Figure S2 in Supplement 1 and Table T4 in Supplement 2. For the generalization and combined analyses, self-reported ancestry was also included as a covariate. Bonferroni corrections were used to account for multiple testing, and the standard genome-wide association study (GWAS) significance threshold for a single trait was further adjusted for 10 amygdala regions considering 9 nuclei volumes and whole amygdala volume ($\alpha = 5 \times 10^{-9}$). Lastly, given the small sample size of the replication analyses, we performed an exact binomial test to investigate whether significant findings would be replicated en masse between the primary and generalization analyses (Supplementary note 2 in Supplement 1).

Genome-wide Association Analyses

After quality control, 31,690 participants and 12,245,112 SNPs remained in the primary (European-only) dataset; 4662 participants and 9,915,367 SNPs remained in the generalization (transancestry) analysis; and 36,352 participants and 9,915,367 SNPs remained in the combined analysis (Table T1 in Supplement 2 and see Supplementary note 3 in Supplement 1 for an extended discussion of the inclusion of diverse ancestries). Seventy-seven percent of the generalization dataset consisted of self-reported European participants, who were significantly different from most of the self-reported Europeans based on principal component analysis, and 23% of participants who self-reported as either South Asian, East Asian, African, mixed, or other ancestries (Table T5 in Supplement 2). GWASs were performed as mega-analyses, with the generalized additive model–residualized amygdala and nuclei volume estimates, using PLINK (version 1.9). Loci were defined with $r^2 > 0.1$ and a genomic window of 250 kb, which were deemed significant after correction for multiple testing ($p < 5 \times 10^{-9}$).

Functional Annotation

The Functional Mapping and Annotation of Genome-Wide Association Studies (FUMA) platform was used to annotate the GWAS results with default settings (25). FUMA maps the top SNP associations to genes based on position. Subsequently, through hypergeometric testing, these genes were investigated for enrichment of biological processes, tissue, cell types, and previous association with traits in the GWAS catalog.

SNP-Based Heritability

Genome-wide complex trait analysis (GCTA) (26) was used to calculate the SNP-based heritability in the European analysis for each generalized additive model–residualized nuclei volume estimate and additional subcortical regions of interest. Other subcortical regions were included as validation to be compared with previous findings. GCTA uses a restricted maximum likelihood approach using individual-level data. Regions with high linkage disequilibrium were pruned before analysis, using a sliding window approach with a window size of 50, a step size of 5, and an r^2 of 0.2. An adjustment for cryptic relatedness was also applied with a threshold of 0.05 (27), excluding 1081 participants from the European analysis. We performed a simple linear regression to test whether heritability estimates and nucleus volumes were correlated. Furthermore, to validate the estimates from GCTA, SNP-based heritability was calculated using linkage disequilibrium score regression (LDSC) (28).

Genetic Correlation and Overlap Between the Nuclei, Other Subcortical Brain Regions, and Psychiatric Traits

The summary statistics from the European analyses were used to determine the genetic correlation between the amygdala nuclei and select subcortical volumes using cross-trait LDSC within the UKB (29). Bivariate MiXeR (version 1.3) was then used to quantify the polygenic overlap between the nuclei (30). Cross-trait LDSC was also used to determine the genetic correlation between the primary analysis of whole amygdala volume and the previous GWAS of whole amygdala volume by Satizabal *et al.* (4). We used conjunctional false discovery rate analysis (31) to identify overlapping genetic loci and cross-trait LDSC to estimate genetic correlations between the nuclei and various psychiatric traits. To maintain independence between the datasets, summary statistics from European analyses that did not include data from the UKB were obtained for alcohol dependence (32), Alzheimer's disease (excluding the *APOE* locus) (33), autism spectrum disorder (ASD) (34), anxiety (35), bipolar disorder (36), Parkinson's disease (37), and schizophrenia (38). These traits were selected based on their associations with genes mapped to the nuclei volumes in the FUMA GWAS catalog and have previously been associated with altered amygdala volumes (39). Lastly, we performed a sensitivity analysis using cross-trait LDSC to determine the genetic correlation between our primary European analyses and an independent analysis that excluded individuals with self-reported neurological or psychiatric conditions (based on field code 2002, $n = 4242$).

Estimating Polygenicity, Discoverability, Power, and Residual Inflation

We used univariate MiXeR (version 1.3) (30,40) to estimate the proportion of causally associated SNPs (polygenicity), the effect size variance (discoverability), the power to detect causal variants, and elevation of z scores due to residual inflation. This model utilizes GWAS summary statistics and the detailed linkage disequilibrium structure of a reference panel and assumes a Gaussian distribution of effect sizes at a fraction of SNPs randomly distributed across the autosomal genome. Based on how closely the data follow the predicted model in the quantile-quantile plots (Figure S3 in Supplement 1) and the positive Akaike information criterion values (Table T6 in Supplement 2), the additional complexity of the MiXeR model more accurately captures the underlying genetic architecture as compared with LDSC (30,40). All z score estimates were close to 1, indicating minimal global inflation.

RESULTS

SNP-Based Heritability

Heritability estimates for the European dataset, determined using GCTA, were all statistically significant ($p < 1 \times 10^{-16}$) (Figure 2A; Table T7 in Supplement 2). The heritability estimate

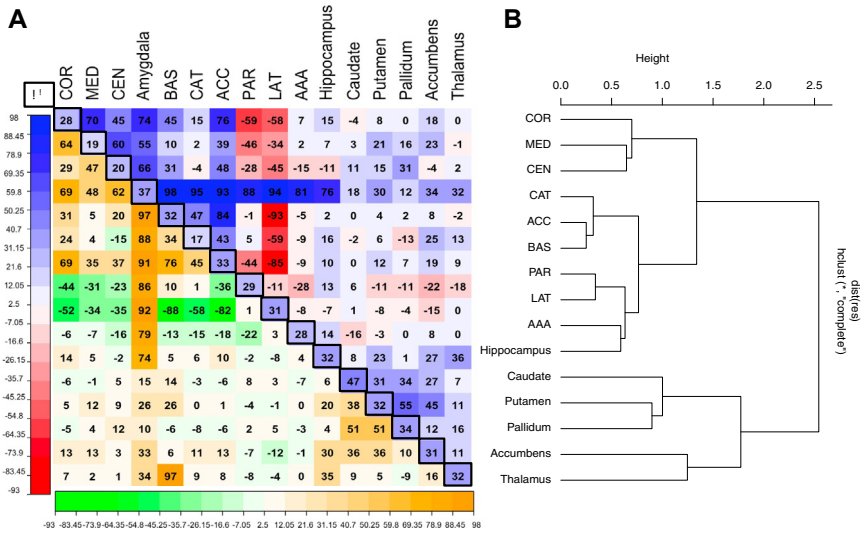

Figure 2. Correlation matrix of the volume estimates for the nuclei as well as several other subcortical regions of interest. **(A)** All correlations are multiplied by a factor of 100. The volumetric correlations are shown in the lower triangle of the matrix (green-orange), the heritability estimates on the diagonal, and the genetic correlations in the upper triangle (blue-red). This heatmap was generated using *corrplot* (2) in R (version 3.6). **(B)** The order, indicated by the dendrogram on the left, was determined by hierarchical clustering using Ward's D2 method. AAA, anterior amygdaloid area; ACC, accessory basal nucleus; BAS, basal nucleus; CAT, corticoamygdaloid transition area; CEN, central nucleus; COR, cortical nucleus; LAT, lateral nucleus; MED, medial nucleus; PAR, paralaminar nucleus.

for whole amygdala volume was 0.37. The heritability estimates for the nuclei volumes ranged from 0.17 for the corticoamygdaloid transition area to 0.33 for the accessory basal nucleus. The heritability estimates determined with LDSC (Table T7 in Supplement 2) were approximately 37% lower than those estimated with GCTA, which is consistent with previous reports (41) (Supplementary note 4 in Supplement 1).

GWAS of the Amygdala Nuclei Volumes

The European analysis of whole amygdala volume identified 8 independent genome-wide significant loci (Table 1; Figure S4 in Supplement 1; Table T8 in Supplement 2), of which 7 loci were novel. The genetic correlation with the GWAS of amygdala volume conducted by Satizabal *et al.* (4) was very high and significant (r_g = 1.01, SE = 0.09, p = 2.59 × 10^{-27}), suggesting shared genetic signals across the datasets. The GWAS for the nuclei volumes identified an additional 21 novel significant loci. Most of the significantly associated loci were unique to specific nuclei (Figure S5 in Supplement 1) and were predominantly intergenic or intronic.

The generalization analysis identified a genome-wide significant locus for central nucleus volume (rs13135092 on chromosome 4), replicating that which was identified in the European analysis (Figure S6 in Supplement 1; Table T8 in Supplement 2). For most nuclei, all independent significant SNPs from the European analysis that were available in the generalization analysis had the same direction of effect. The binomial test indicated that this was significantly different from chance for the central nucleus (p = .03) and whole amygdala volume (p = .01) (Supplementary note 2 in Supplement 1).

The combined GWAS of whole amygdala volume identified 10 significant loci (Figure S7 in Supplement 1; Table T8 in Supplement 2). Of these, 7 loci were shared with the European analysis. An additional 29 significant loci, 25 of which were also observed in the European analysis, were identified across the 9 nuclei volumes. A consistent direction of allelic effect was observed across the significant loci shared with the European analysis results.

Functional Annotation

In the European analysis, across the whole amygdala and the 9 nuclei, 1436 genes were mapped to significant loci, 588 of which were protein coding (Table T9 in Supplement 2). Hypergeometric tests, performed as part of the *gene2func* in FUMA, identified biological processes associated with the genes mapped to the whole amygdala, basal, central, and medial nucleus volumes (Table T10 in Supplement 2). Immune-related pathways were associated across basal and central nucleus volumes (e.g., defense response to Gram positive bacteria) (p_{adj} = 1.38 × 10^{-5}). DNA modification pathways, circadian rhythms, and lipoprotein clearance were associated with the genes mapped to the central and basal nucleus (e.g., nucleosome organization) (p_{adj} = 2.22 × 10^{-43}), medial nucleus (e.g., regulation of hormone secretion) (p_{adj} = 8.27 × 10^{-5}), and whole amygdala volumes (e.g., very-low-density lipoprotein particle clearance) (p_{adj} = 1.24 × 10^{-6}), respectively.

Furthermore, to determine whether any of the GWAS hits had previously been associated with other disorders or traits, the mapped genes were also compared against the GWAS catalog in FUMA (Table T11 in Supplement 2). Most of the genes/loci across the nuclei had previously been associated with psychiatric and behavioral traits, e.g., ASD and basal nucleus volume (p_{adj} = 6.88 × 10^{-182}) and cardiovascular traits such as blood pressure with central nucleus volume (p_{adj} = 2.68 × 10^{-5}). In addition, the identified genes had previously been associated with the hippocampus and its subfield volumes, e.g., paralaminar nucleus volume (hippocampal subfield CA1 volume, p_{adj} = 5.17 × 10^{-9}).

Table 1. Genome-wide Significant Loci for the Whole Amygdala and Nuclei Volumes From the European Analysis

Region of Interest	Unique Locus	Lead SNP	A1	MAF	Chr	Start (BP)	End (BP)	β	*p* Value	Number of Significant SNPs	Nearest Gene(s)
Whole Amygdala (282 Significant SNPs, 287 Genes)	1	rs33931638	A	0.08	1	46317219	46587530	−27.59	1.44×10^{-9}	6	*MAST2*, *PIK3R3*
	2	rs58531798	G	0.40	3	190591418	190678743	17.86	8.54×10^{-13}	162	*GMNC*
	3	rs13131500	G	0.10	4	103188709	103387094	27.84	4.14×10^{-10}	14	*SLC39A8*, *RP11-499E18.1*, *AF213884.1*
	4	rs4947122	T	0.24	6	111870090	111870090	−17.92	3.6×10^{-9}	1	*TRAF3IP2*
	5	rs1419859	T	0.38	12	4004752	4013260	−25.59	1.7×10^{-24}	11	*RP11-664D1.1*
	6	rs17178006	G	0.08	12	65463647	65874956	−31.62	2.05×10^{-17}	45	*MSRB3*, *KRT18P60*, *WIF1*, *RP11-305O6.3*, *RP11-230G5.2*
	7	rs11068224	A	0.09	12	117309440	117506632	34.53	8.78×10^{-15}	38	*HRK*, *FBXW8*, *TESC*, *RP11-240G22.1*
	8	rs10414043	A	0.12	19	45410002	45421254	−23.15	2.2×10^{-10}	5	*APOE*, *APOC1*
Anterior Amygdaloid Area (233 Significant SNPs, 189 Genes)	3	rs13107325	T	0.08	4	102707791	103388441	−1.77	5.48×10^{-41}	108	*BANK1*, *RP11-498M5.2*, *SLC39A8*, *RP11-499E18.1*, *AF213884.1*
	9	rs12667816	C	0.16	7	83644954	83705871	−0.58	5.54×10^{-10}	22	*SEMA3A*
	10	rs17734690	C	0.49	8	9042454	10286532	0.44	6.23×10^{-11}	65	*TNKS*, *snoU13*, *MSRA*, *RP11-10A14.6*
	11	rs28629854	G	0.32	9	98259703	98299677	−0.44	1.11×10^{-9}	8	*PTCH1*
Accessory Basal Nucleus (44 Significant SNPs, 71 Mapped Genes)	12	rs6658111	G	0.36	1	47940080	47984381	1.44	9.94×10^{-16}	12	*RP4-666O22.3*, *RPL21P24*, *AL356458.1*
	13	rs116472807	T	0.05	1	183030814	183030814	2.30	3.11×10^{-9}	1	*LAMC1*
	3	rs13107325	T	0.08	4	102865304	103387161	3.54	7.58×10^{-26}	31	*SLC39A8*, *BANK1*, *RP11-498M5.2*, *AF213884.1*
Basal Nucleus (186 Significant SNPs, 280 Mapped Genes)	12	rs12118339	C	0.36	1	47984143	47984143	−1.46	3.17×10^{-9}	1	*AL356458.1*
	14	rs11903299	G	0.34	2	105405557	105473698	−1.77	1.22×10^{-12}	43	*POU3F3*, *RP11-13J10.1*, *HMGB3P11*, *LINC01158*
	15	rs79072812	C	0.23	3	69303968	69338070	−1.77	4.12×10^{-10}	11	*FRMD4B*
	16	rs58825580	G	0.12	6	26354780	26365759	2.03	2.52×10^{-9}	4	*RNU6-1259P*, *BTN3A2*, *AL021917.1*
	17	rs13197176	T	0.07	6	27698837	28368508	2.22	2.04×10^{-9}	66	*RP1-97D16.1*, *RSL24D1P1*, *HIST1H4L*, *HIST1H3J*, *RNU7-26P*, *OR2B2*, *OR2W6P*, *RPLP2P1*, *OR2W4P*, *IQCB2P*, *U3*, *OR2W2P*, *OR2B7P*, *OR1F12*, *ZSCAN12P1*, *RP1-265C24.5*, *ZSCAN16-AS1*, *ZKSCAN8*, *ZNF192P1*, *ZNF192P2*, *PGBD1*, *RP5-874C20.6*, *ZSCAN31*
	18	rs12377595	G	0.26	9	126326884	126684733	2.08	1.16×10^{-13}	61	*DENND1A*, *RP11-417B4.2*

Table 1. Continued

Region of Interest	Unique Locus	Lead SNP	A1	MAF	Chr	Start (BP)	End (BP)	β	*p* Value	Number of Significant SNPs	Nearest Gene(s)
Corticoamygdaloid Transition Area (13 Significant SNPs, 32 Mapped Genes)	12	rs61784835	T	0.36	1	47940080	47984143	1.10	4.47×10^{-15}	12	*RP4-666O22.3*, *RPL21P24*, *AL356458.1*
	19	rs12146713	C	0.09	12	106476805	106476805	−1.51	4.08×10^{-11}	1	*NUAK1*
Central Nucleus (378 Significant SNPs, 198 Genes)	20	rs6667291	A	0.47	1	180943529	181017348	−0.55	2.64×10^{-12}	42	*RP11-46A10.5*, *AL162431.1*, *STX6, MR1*
	21	rs34722008	A	0.29	4	38602202	38691024	−0.56	4.02×10^{-12}	19	*RP11-617D20.1*, *AC021860.1*, *KLF3*
	3	rs13107325	T	0.08	4	102638020	103388441	2.93	1.26×10^{-84}	131	*BANK1*, *SLC39A8*, *RP11-498M5.2*, *RP11-499E18.1*, *AF213884.1*
	22	rs149359690	T	0.07	6	25526319	25582712	−0.77	1.94×10^{-9}	3	*LRRC16A*
	23	rs6558056	G	0.49	8	22226081	22294836	−0.56	4.94×10^{-13}	63	*SLC39A14*, *RNU6-336P*
	24	rs7154495	C	0.42	14	100223304	100269887	0.52	5.35×10^{-11}	16	*EML1*
Cortical Nucleus (34 Significant SNPs, 69 Mapped Genes)	12	rs6658111	G	0.36	1	47974123	47984143	0.33	8.05×10^{-17}	4	*AL356458.1*
	25	rs2372785	C	0.43	2	37075013	37152899	−0.24	7.31×10^{-10}	10	*STRN*
	3	rs13107325	T	0.08	4	102865304	103376409	0.64	1.72×10^{-18}	20	*BANK1*, *SLC39A8*, *RP11-498M5.2*, *RP11-499E18.1*
Lateral Nucleus (126 Significant SNPs, 128 Genes)	12	rs12118339	C	0.36	1	47945825	47984143	2.47	9.19×10^{-12}	10	*RP4-666O22.3*, *RPL21P24*, *AL356458.1*
	13	rs116472807	T	0.05	1	183030814	183030814	−4.63	5.35×10^{-9}	1	*LAMC1*
	3	rs13107325	T	0.08	4	102926923	103292422	−5.97	4.49×10^{-18}	14	*BANK1*, *SLC39A8*, *RP11-498M5.2*
	18	rs12377595	G	0.27	9	126329270	126,654,811	−2.79	1.31×10^{-11}	33	*DENND1A*
	26	rs748609	C	0.37	19	18533642	18631332	2.24	8.82×10^{-10}	68	*ELL*, *SSBP4*, *ISYNA1*, *CTD-3137H5.1*
Medial Nucleus (183 Significant SNPs, 78 Mapped Genes)	27	rs11133400	G	0.34	4	56291479	56455791	0.40	4.24×10^{-11}	146	*TMEM165*, *CLOCK*, *PDCL2*, *NMU*, *RP11-528I4.2*
	3	rs13107325	T	0.08	4	102707791	103387161	1.18	2.42×10^{-25}	37	*BANK1*, *SLC39A8*, *RP11-498M5.2*, *RP11-499E18.1 AF213884.1*
Paralaminar Nucleus (39 Significant SNPs, 105 Mapped Genes)	28	9:139980417_T_C	T	0.33	9	139957982	140003844	−0.32	1.06×10^{-13}	22	*MAN1B1*, *UAP1L1*, *SAPCD2*, *AL807752.1*, *DPP7*, *ENTPD2*
	7	rs7137149	C	0.11	12	117319202	117332156	0.42	4.18×10^{-11}	10	*HRK*
	29	rs6120844	T	0.11	20	33717245	33720240	−0.40	1.08×10^{-9}	7	*EDEM2*

A1, effect allele; BP, base pair; Chr, chromosome; MAF, minor allele frequency; SNP, single nucleotide polymorphism.

Genetic Overlap and Correlations Between Nuclei, Other Subcortical Regions, and Psychiatric Disorders

The volumetric correlations broadly mirrored the genetic correlations, determined with LDSC, between each nucleus' volume and additional subcortical regions (Figure 2A). The genetic correlations further revealed two primary clusters using Ward's D2 minimum variance hierarchical clustering method (42) (Figure 2B). The first cluster consisted of the whole amygdala, the amygdala nuclei, and hippocampus volumes. The second cluster included the basal ganglia and the thalamus.

Furthermore, the extent of shared polygenicity, determined with bivariate MiXeR, indicated both shared and unique effects between the nuclei (Figure 3; Figure S8 in Supplement 1; Table T12 in Supplement 2). Across the nuclei, central nucleus volume had the lowest Dice coefficients, indicating a large degree of unique genetic effects. The cortical nucleus had the highest Dice coefficients, suggesting that it shared the largest proportion of associated variants with other nuclei.

Conjunctional false discovery rate analysis revealed significant overlap between ASD and anterior amygdaloid transition area volume; Alzheimer's disease and whole amygdala, accessory basal, and basal and lateral nuclei volumes; bipolar disorder and basal and lateral nuclei volumes; Parkinson's disease and anterior amygdaloid transition area, cortico-amygdaloid transition area, and cortical, medial and paralaminar nuclei volumes; and schizophrenia and all nuclei volumes except for the paralaminar nucleus volume (Table 2; Figure S9 in Supplement 1). A mixed pattern of allelic effect directions was observed across these overlapping loci, i.e., was associated with larger and smaller nuclei volumes. LDSC revealed a significant genetic correlation between Alzheimer's disease and whole amygdala volume, ASD and lateral and accessory basal nucleus volumes, and schizophrenia and anterior amygdaloid transition area volume (Table T13 in Supplement 2).

Lastly, the genetic correlation between the primary European analyses and an independent analysis with the 4242 individuals with a self-reported neurological or psychiatric diagnosis excluded was high ($r_g > .99$) (Table T14 in Supplement 2). This suggests that the exclusion of these individuals did not influence the genetic signal across either the whole amygdala or any of the nuclei, and so they were retained in our analyses.

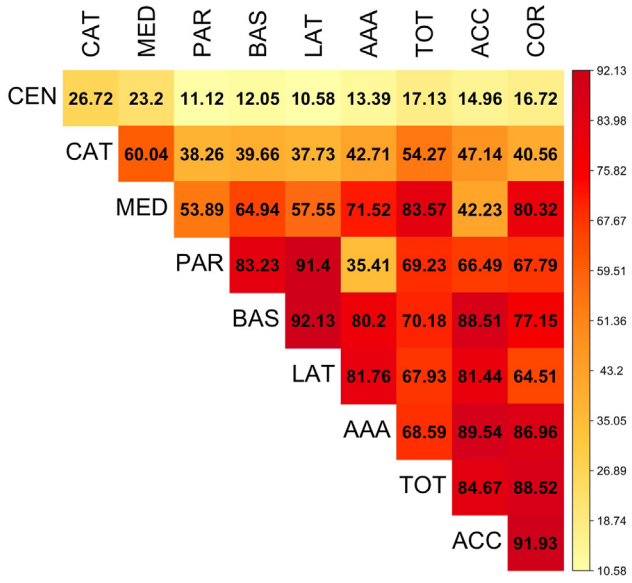

Figure 3. Heatmap of the estimated proportion of shared variants between amygdala nuclei volumes. The heatmap illustrates the Dice coefficients between the amygdala nuclei volumes as determined by bivariate MiXeR, which indicate what proportion of the nuclei on the x-axis is shared with the nuclei on the y-axis. The order in which the nuclei appear on the heatmap was determined by hierarchical clustering using Ward's D2 method. This heatmap was generated using *corrplot* (2) in R (version 3.6). AAA, anterior amygdaloid area; ACC, accessory basal nucleus; BAS, basal nucleus; CAT, corticoamygdaloid transition area; CEN, central nucleus; COR, cortical nucleus; LAT, lateral nucleus; MED, medial nucleus; PAR, paralaminar nucleus; TOT, whole amygdala.

Polygenicity, Discoverability, Power, and Residual Inflation

The polygenicity and discoverability estimates were mainly on the same order of magnitude across the nuclei, except for the paralaminar nucleus. The paralaminar nucleus volume had the lowest polygenicity and the central nucleus volume had the highest polygenicity overall (Table T6 in Supplement 2). An inverse relationship was observed for discoverability.

The current analyses accounted for <1% of the estimated variance for all the nuclei except for the whole amygdala (1.4% and 1.8%) and central nucleus (16.1% and 26%) volumes in the European and combined-ancestry participants, respectively (Figure 4). Only the central nucleus volume captured more genetic variance than the whole amygdala volume. Gains in power were observed for the whole amygdala volume and the accessory basal, basal, central, cortical, medial, and lateral nuclei in the combined ancestry compared with the European analysis. Using current methods, the power curve further suggested that an effective population size of 10 million samples would be required to capture the full genetic variance of each nucleus.

DISCUSSION

We identified 29 genome-wide significant loci associated across the whole amygdala and amygdala nucleus volumes in ~32,000 individuals of European ancestry and an additional 10 loci when including ~5000 individuals of various other ancestries. As evidenced by the genome-wide significant loci, genetic correlation, and overlap, much of the genetic architecture is shared across the nuclei, as reflected by the high level of collinearity across their volumes. Furthermore, we showed that altered amygdala nuclei volumes shared genetic overlap with specific brain disorders. Lastly, we showed that the segmentation algorithm did influence our findings, which need to be interpreted accordingly.

The genetic correlation between our GWAS of whole amygdala volume and that of Satizabal *et al.* (4) was high and significant. We also replicated the previously reported genome-wide significant locus associated with amygdala volume (rs17178006 on chromosome 12) (4). This locus spans

Table 2. Variants With Significant Shared Effects Across the Amygdala Nuclei Volumes and Select Psychiatric Traits

Trait 1	Trait 2	Locus	SNP	Chr	BP	A1	A2	Mapped Gene(s)	*p* Value Trait 1	*p* Value Trait 2	FDR Trait 1	conjFDR for Trait 1 and Trait 2	minimum conjFDR	*Z* Score Trait 1	*Z* Score Trait 2
Alzheimer's Disease	ACC	1	rs748609	19	18560282	C	T	*ELL, AC010335.2, AC010335.3*	4.35×10^{-5}	1.78×10^{-5}	9.61×10^{-2}	9.74×10^{-3}	9.74×10^{-3}	4.09	−4.29
	BAS	1	rs10408290	19	18542701	T	C	*SSB4*	2.53×10^{-5}	5.78×10^{-7}	6.64×10^{-2}	6.21×10^{-3}	6.21×10^{-3}	4.21	−5.00
	LAT	1								4.76×10^{-9}		6.54×10^{-3}	6.54×10^{-3}		5.86
	TOT	1	rs269776	5	139475287	A	G	*MALINC1*	4.08×10^{-6}	1.17×10^{-5}	1.85×10^{-2}	4.54×10^{-3}	4.54×10^{-3}	−4.61	−4.38
Autism Spectrum Disorder	AAA	1	rs4840484	8	10297049	C	T	*AC104964.2*	6.29×10^{-6}	1.32×10^{-6}	3.28×10^{-1}	1.38×10^{-3}	1.38×10^{-3}	4.52	−4.84
Bipolar Disorder	BAS	1	rs72906804	1	51450144	G	A	–	9.65×10^{-6}	1.15×10^{-5}	2.12×10^{-2}	5.48×10^{-3}	5.48×10^{-3}	4.42	−4.39
	LAT	1	rs57331401	1	51451372	A	G	–	7.36×10^{-6}	6.14×10^{-6}	1.83×10^{-2}	2.91×10^{-3}	2.91×10^{-3}	−4.48	4.52
Parkinson's Disease	AAA	1	rs2979160	8	8307666	G	A	–	7.64×10^{-6}	4.83×10^{-8}	1.30×10^{-2}	1.66×10^{-3}	1.66×10^{-3}	−4.48	−5.46
	CAT	1	rs62062797	17	44027366	G	T	*MAPT*	2.61×10^{-24}	1.18×10^{-5}	2.64×10^{-7}	4.03×10^{-3}	4.03×10^{-3}	10.17	−4.38
	CEN	1	rs1293290	8	11709957	C	T	*CTSB*	1.72×10^{-6}	1.98×10^{-5}	3.15×10^{-3}	8.13×10^{-3}	8.13×10^{-3}	4.78	4.27
	COR	1	rs12413409	10	104719096	A	G	*CNNM2*	1.18×10^{-6}	4.13×10^{-6}	2.44×10^{-3}	1.37×10^{-3}	1.37×10^{-3}	−4.86	4.60
		2	rs79780963	10	104952499	T	C	*NT5C2*	2.02×10^{-5}	2.27×10^{-5}	3.05×10^{-2}	6.60×10^{-3}	6.60×10^{-3}	4.26	−4.24
	MED	1	rs12413409	10	104719096	A	G	*CNNM2*	1.18×10^{-6}	2.75×10^{-6}	2.68×10^{-3}	8.05×10^{-4}	8.05×10^{-4}	−4.86	4.69
		1	rs79780963	10	104952499	T	C	*NT5C2*	2.02×10^{-5}	6.47×10^{-6}	3.23×10^{-2}	4.58×10^{-3}	4.58×10^{-3}	4.26	−4.51
	PAR	1	rs199500	17	44863413	T	C	*WNT3*	2.62×10^{-20}	5.85×10^{-6}	2.65×10^{-7}	2.24×10^{-3}	2.24×10^{-3}	−9.23	4.53
Schizophrenia	AAA	1	rs35225200	4	103146888	C	A	–	3.57×10^{-11}	6.99×10^{-28}	9.52×10^{-7}	3.36×10^{-8}	3.36×10^{-8}	6.62	−10.95
		2	rs1994224	8	9966586	G	A	*MSRA*	9.15×10^{-6}	1.98×10^{-5}	5.55×10^{-3}	6.33×10^{-3}	6.33×10^{-3}	4.44	−4.27
		2	rs11249996	8	10245463	C	A	*MSRA*	2.55×10^{-6}	9.25×10^{-10}	2.26×10^{-3}	6.81×10^{-4}	6.81×10^{-4}	4.70	−6.12
		3	rs9910849	17	2175768	T	C	*SMG6*	2.04×10^{-5}	2.71×10^{-5}	9.52×10^{-3}	8.49×10^{-3}	8.49×10^{-3}	4.26	4.20
	ACC	1	rs7515178	1	205084120	A	G	*RBBP5*	2.14×10^{-5}	2.38×10^{-5}	9.86×10^{-3}	8.31×10^{-3}	8.31×10^{-3}	4.25	4.23
		2	rs35225200	4	103146888	C	A	–	3.57×10^{-11}	1.03×10^{-17}	9.15×10^{-7}	4.86×10^{-8}	4.86×10^{-8}	6.62	8.57
		3	rs629444	6	25885814	T	C	*AL138726.1*	8.43×10^{-12}	6.48×10^{-6}	9.15 sd^{-7}	2.43×10^{-3}	2.43×10^{-3}	6.83	4.51
		4	rs57070985	19	4969053	G	A	*KDM4B*	2.11×10^{-5}	7.06×10^{-6}	9.76×10^{-3}	4.99×10^{-3}	4.99×10^{-3}	4.25	−4.49
	BAS	1	rs13135092	4	103198082	G	A	*SLC39A8*	1.12×10^{-10}	1.32×10^{-8}	1.14×10^{-6}	8.35×10^{-6}	8.35×10^{-6}	6.45	5.68
		2	rs9295675	6	25918473	T	A	*SLC17A2*	1.17×10^{-12}	3.51×10^{-8}	1.03×10^{-6}	2.27×10^{-5}	2.27×10^{-5}	7.11	5.51
		3	rs4144686	18	53251725	A	G	*TCF4*	4.14×10^{-8}	1.26×10^{-6}	1.17×10^{-4}	8.85×10^{-4}	8.85×10^{-4}	5.48	−4.85
	CAT	1	rs11709284	3	52559705	G	A	*STAB1, NT5DC2*	1.79×10^{-5}	9.22×10^{-6}	8.69×10^{-3}	6.34×10^{-3}	6.34×10^{-3}	4.29	−4.43
	CEN	1	rs35225200	4	103146888	C	A	–	3.57×10^{-11}	3.58×10^{-59}	9.48×10^{-7}	4.29×10^{-8}	4.29×10^{-8}	6.62	16.22
		2	rs4702	15	91426560	G	A	*FES, FURIN*	8.54×10^{-11}	3.18×10^{-5}	9.48×10^{-7}	9.34×10^{-3}	9.34×10^{-3}	6.49	−4.16

Table 2. Continued

Trait 1	Trait 2	Locus	SNP	Chr	BP	A1	A2	Mapped Gene(s)	*p* Value Trait 1	*p* Value Trait 2	FDR Trait 1	conjFDR for Trait 1 and Trait 2	minimum conjFDR	*Z* Score Trait 1	*Z* Score Trait 2
	COR	1	rs1366837	2	198160501	C	T	*ANKRD44, ANKRD44-IT1*	7.16×10^{-7}	4.37×10^{-7}	8.82×10^{-4}	1.77×10^{-4}	1.77×10^{4}	4.96	5.05
		2	rs35225200	4	103146888	C	A	–	3.57×10^{-11}	3.88×10^{-13}	9.34×10^{-7}	4.90×10^{-8}	4.90×10^{-8}	6.62	7.26
		3	rs2980763	8	8311477	G	T	–	3.48×10^{-5}	1.26×10^{-5}	1.40×10^{-2}	4.80×10^{-3}	4.80×10^{-3}	4.14	−4.37
		4	rs150786824	10	104612941	A	G	*AL358790.1, BORCS7, BORCS7-ASMT*	4.55×10^{-11}	1.87×10^{-6}	9.34×10^{-7}	6.76×10^{-4}	6.76×10^{-4}	6.58	4.77
		4	rs79780963	10	104952499	T	C	*NT5C2*	3.19×10^{-14}	2.09×10^{-5}	9.34×10^{-7}	5.96×10^{-3}	5.96×10^{-3}	−7.59	−4.25
	LAT	1	rs7515178	1	205084120	A	G	*RBBP5*	2.14×10^{-5}	1.70×10^{-5}	9.91×10^{-3}	7.37×10^{-3}	7.37×10^{-3}	4.25	−4.30
		2	rs35225200	4	103146888	G	A	–	3.57×10^{-11}	2.55×10^{-11}	1.06×10^{-6}	5.48×10^{-8}	5.48×10^{-8}	6.62	−6.67
		3	rs629444	6	25885814	T	C	*AL138726.1*	8.43×10^{-12}	6.43×10^{-7}	1.06×10^{-6}	3.01×10^{-4}	3.01×10^{-4}	6.83	−4.98
	MED	1	rs35225200	4	103146888	C	A	–	3.57×10^{-11}	2.82×10^{-18}	9.48×10^{-7}	4.16×10^{-8}	4.16×10^{-8}	6.62	8.72
		2	rs999867	10	104504564	T	C	*SFXN2, WBP1L*	2.42×10^{-7}	2.52×10^{-5}	4.06×10^{-4}	7.94×10^{-3}	7.94×10^{-3}	5.16	4.21
		2	rs284855	10	104574422	A	G	*WBP1L*	4.79×10^{-8}	1.81×10^{-6}	1.29×10^{-4}	6.31×10^{-4}	6.31×10^{-4}	5.46	4.77
		2	rs79780963	10	104952499	T	C	*NT5C2*	3.19×10^{-14}	6.18×10^{-6}	9.48×10^{-7}	2.07×10^{-3}	2.07×10^{-3}	−7.59	−4.52
	TOT	1	rs1896293	2	60718848	T	G	*BCL11A*	3.10×10^{-5}	1.52×10^{-5}	1.29×10^{-2}	7.47×10^{-3}	7.47×10^{-3}	4.17	4.33
		2	rs13107325	4	103188709	T	C	*SLC39A8*	5.38×10^{-11}	1.37×10^{-9}	9.44×10^{-7}	9.10×10^{-7}	9.10×10^{-7}	6.56	6.06
		3	rs4788190	16	29948401	G	A	–	4.83×10^{-9}	6.31×10^{-7}	2.34×10^{-5}	3.73×10^{-4}	3.73×10^{-4}	5.85	4.98

A1, effect allele; A2, alternative allele; AAA, anterior amygdaloid area; ACC, accessory basal nucleus; BAS, basal nucleus; BP, base pair position; CAT, corticoamygdaloid transition area; CEN, central nucleus; Chr, chromosome; conjFDR, conjunctional false discovery rate analysis; COR, cortical nucleus; LAT, lateral nucleus; MED, medial nucleus; PAR, paralaminar nucleus; TOT, whole amygdala; SNP, single nucleotide polymorphism.

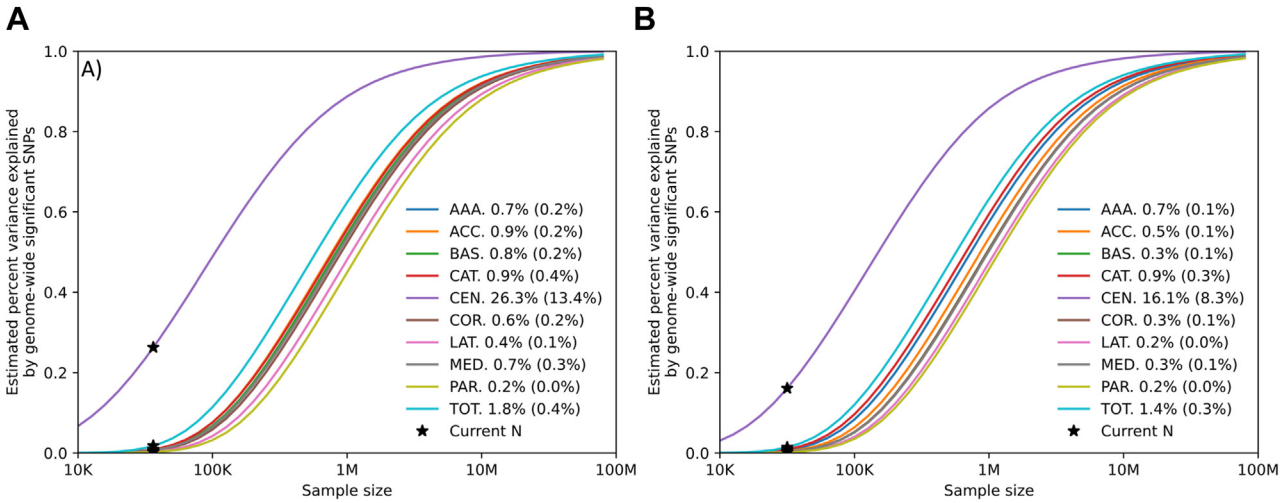

Figure 4. MiXeR power curves and model fit for all amygdala nuclei volumes from the European and combined analyses. **(A)** and **(B)** refer to the power curves for the whole amygdala and its nuclei for the European and combined analyses, respectively. This figure depicts the sample size required so that a given proportion of phenotypic variability is captured by significant SNPs for the nuclei volumes. Each curve on the plot represents a different nucleus, and the right-to-left curve is determined by decreasing discoverability. The proportion of phenotypic variance explained is shown in brackets next to the corresponding nucleus volume in the legend. AAA, anterior amygdaloid area; ACC, accessory basal nucleus; BAS, basal nucleus; CAT, corticoamygdaloid transition area; CEN, central nucleus; COR, cortical nucleus; LAT, lateral nucleus; MED, medial nucleus; PAR, paralaminar nucleus; SNP, single nucleotide polymorphism; TOT, whole amygdala.

an intronic region that has been associated with several psychiatric phenotypes including cognitive performance (43) and bipolar disorder (44). The previous amygdala volume GWAS (4) had approximately the same number of study participants as the current study; however, we identified many more variants. First, this discrepancy may be due to the nature of mega- versus meta-analyses, which have equal power only under strict conditions (45). Second, Satizabal *et al.* (4) combined data from 3 distinct consortia, with European participants from across the globe of varying age ranges (9–90 years). The UKB samples were sourced from the same geographical location, included only adult participants (44–82 years), and used the same recruitment approaches and methodology across all participants (19,20,46). Including a limited age range, consistent methodology, and European participants from the same country significantly reduces sample heterogeneity, thereby allowing for greater power to detect associated variants.

However, the homogeneity of the European UKB participants may reduce the generalizability of our findings; therefore, we included individuals of various ancestries, which are typically excluded in these types of analyses, in our generalization and combined analyses (47). The generalization analyses replicated a significant locus for the central nucleus (rs13135092 on chromosome 4) and showed en masse replication for the central nucleus and whole amygdala volume. Despite individuals from the generalization analysis accounting for only 15% of the combined analysis and the loss of ~2 million SNPs, we identified 10 additional candidate loci and found additional support for 25 loci identified in the European-only analysis, in which most loci improved in statistical significance. The additional samples may have boosted power, although this is unlikely given the fact that introducing sample heterogeneity typically has the opposite effect (48). The boost in power that was observed here is likely due to a combination of increased sample size and the relatively higher minor allele frequencies of most of these additional loci in non-European populations (https://www.ensembl.org/index.html). However, the UKB represents individuals with higher income and education levels and better overall health than the general population in the United Kingdom (49). Therefore, even when including individuals across ancestries, this sample may not be representative of the general population, and additional replication samples are required to investigate the generalizability of and replicate our findings across ancestry, age, and sociodemographic groups.

Immune-related pathways were associated with the genes mapped across several nuclei, particularly the central nucleus volume. The brain has a resident immune system that interacts with peripheral immunity and impacts behavior (50). Many of the psychiatric disorders that share overlapping loci with the nuclei volumes, e.g., schizophrenia (51), ASD (52), and anxiety and mood disorders (53,54), have immune dysfunction as a component of their etiology. Animal models have demonstrated that maternal immune activation during pregnancy significantly affects brain development and is a risk factor for many neurological disorders (55). The resident immune and immune-related cells in the brain affect synaptic and myelin formation and pruning throughout the lifespan, thereby affecting brain volume and communication (50). One such resident group of immune cells, the microglia, may directly influence behavior. For example, studies with mice have shown an increased risk for obsessive-compulsive symptoms when microglia are hyperactivated (56) and ASD-like symptoms when microglial signaling is impaired (57). Our findings suggest that these immune pathways may be pertinent to amygdala nuclei structure and function.

With the exception of the central nucleus, the whole amygdala had the highest power for discovery, and genetic correlations across the nuclei were high. SNP-based heritability ranged from 0.17 to 0.33 across the nuclei but was still highest for whole amygdala volume (0.37). Regardless, investigating the nuclei separately revealed an additional 20 candidate loci worthy of follow-up. The central nucleus may be an outlier given its evolutionary context. It is a highly conserved region and is likely under strong genetic influence linked to its role in fear expression and defensive behaviors (5). Furthermore, the central nucleus has been extensively researched compared with the other nuclei (5), which may have resulted in clearly defined structural and functional boundaries. However, it is important to recognize that the central nucleus has a low SNP-based heritability and is one of the smaller nuclei, making segmentation more challenging and prone to error. Therefore, all of these findings need to be considered within the limitations of the segmentation algorithm.

The segmentation algorithm utilized in this study is still relatively new. However, several studies have compared the FreeSurfer segmentation protocol with manual segmentation and the automated segmentations from FIRST and ANTS (58). All the automated segmentations overestimated amygdala nuclei volumes, especially for smaller nuclei, as compared with manual segmentation. However, this overestimation was most subtle for FreeSurfer as compared with the other automated protocols (58). Although we did not observe a correlation between the size of each nucleus and the number of genome-wide significant loci, we did see a correlation with the heritability estimates. Therefore, our findings may be influenced by inherent segmentation errors which must be taken into consideration. A gene expression atlas, which has been incorporated for the hippocampus, may aid noise reduction and amplify power because it utilizes an unbiased molecular approach to define subfield boundaries (59). Furthermore, harmonizing the definitions and segmentation algorithms used in the literature will significantly improve the interpretation and comparison of findings (60).

Overall, we showed that investigating the amygdala with increased power and phenotypic specificity, through segmentation into 9 nuclei, enhanced genetic discoverability despite the large degree of genetic correlation among the nuclei. Across the amygdala and its nuclei, we have identified 28 novel variants in a European-only analysis and 10 additional candidate loci from a combined analysis including trans-ancestry participants. Our findings indicate that the amygdala nuclei have specific associations with biological processes and genetic overlap with brain disorders. Continued efforts are needed to further our understanding of the genes implicated in the genetic architecture of amygdala nuclei. Lastly, these findings need to be considered within the limitations of the automated segmentation, which will need to be refined in future research.

ACKNOWLEDGMENTS AND DISCLOSURES

RAM was supported by the U.S. Department of Veterans Affairs Mid-Atlantic Mental Illness Research, Education, and Clinical Center core funds of the Department of Veterans Affairs Office of Mental Health Services. RAM also received financial support from the Veterans Affairs Office of Research and Development (Grant Nos. 5I01CX000748-01 and 5I01CX000120-02). Additional financial support was provided by the National Institute of Neurological Disorders and Stroke (Grant No. R01NS086885-01A1). MSM is supported by the South African National Research Fund, the David and Elaine Potter Foundation, and the Global Initiative for Neuropsychiatric Genetics Education in Research program. The Global Initiative for Neuropsychiatric Genetics Education in Research program is supported in part by an award from the National Institute of Mental Health (Grant No. 1R01MH120642). TK, DvdM, and OAA are funded by the Research Council of Norway (Grant Nos. 276082, 223273, 275054, and 324499). RR, DJS, and SD are supported by the South African Medical Research Council. This work was partly performed on the Tjeneste for Sensitive Data facilities owned by the University of Oslo, operated and developed by the Tjeneste for Sensitive Data service group at the University of Oslo IT-Department (tsd-drift@usit.uio.no).

A previous version of this article was published as a preprint on medRxiv: https://doi.org/10.1101/2021.06.30.21258615.

All summary statistics are available from https://github.com/norment/open-science. This study used openly available software and code: FreeSurfer, https://surfer.nmr.mgh.harvard.edu/; Plink1.9, https://www.cog-genomics.org/plink/; LDSC, https://github.com/bulik/ldsc/; GCTA, https://yanglab.westlake.edu.cn/software/gcta/; cFDR, https://github.com/precimed/pleiofdr/; MiXeR, https://github.com/precimed/mixer/.

OAA is a consultant to Cortechs.ai and has received speaker's honoraria from Lundbeck, Sunovion, and Janssen, and DJS has received consultancy honoraria from Discovery Vitality, Johnson & Johnson, Kanna, L'Oreal, Lundbeck, Orion, Sanofi, Servier, Takeda, and Vistagen, unrelated to the topic of this study. All other authors report no biomedical financial interests or potential conflicts of interest.

ARTICLE INFORMATION

From the South African Medical Research Council Genomic and Precision Medicine Research Unit, Division of Human Genetics, Department of Pathology, Institute of Infectious Disease and Molecular Medicine, University of Cape Town, Cape Town, South Africa (MSM, RR, SD); Global Initiative for Neuropsychiatric Genetics Education in Research program, Harvard T.H. Chan School of Public Health and the Stanley Center for Psychiatric Research at the Broad Institute of Harvard and MIT, Boston, Massachusetts (MSM); South African Medical Research Council Unit on Risk & Resilience in Mental Disorders, Department of Psychiatry and Neuroscience Institute, University of Cape Town, Cape Town, South Africa (MSM, DJS); Norwegian Centre for Mental Disorders Research Centre, Division of Mental Health and Addiction, Oslo University Hospital & Institute of Clinical Medicine, University of Oslo, Oslo, Norway (DvdM, TK, OF, OAA); School of Mental Health and Neuroscience, Faculty of Health, Medicine and Life Sciences, Maastricht University, Maastricht, the Netherlands (DvdM); Department of Psychiatry and Psychotherapy, Tübingen Center for Mental Health, University of Tübingen, Tübingen, Germany (TK); Center for Bioinformatics, Department of Informatics, University of Oslo, Oslo, Norway (OF); Imaging Genetics Center, Stevens Neuroimaging and Informatics Institute, Keck School of Medicine of the University of Southern California, Marina del Rey, California (PMT, NJ); Duke-UNC Brain Imaging and Analysis Center, Duke University, Durham, North Carolina (RAM); and KG Jebsen Centre for Neurodevelopmental Centre, Institute of Clinical Medicine, University of Oslo, Oslo, Norway (OAA).

Address correspondence to Mary S. Mufford, Ph.D., at mffmar004@myuct.ac.za.

Received Mar 8, 2022; revised and accepted Jun 2, 2023.

Supplementary material cited in this article is available online at https://doi.org/10.1016/j.biopsych.2023.06.022.

REFERENCES

1. Amunts K, Kedo O, Kindler M, Pieperhoff P, Mohlberg H, Shah NJ, *et al.* (2005): Cytoarchitectonic mapping of the human amygdala, hippocampal region and entorhinal cortex: Intersubject variability and probability maps. Anat Embryol (Berl) 210:343–352.
2. Hortensius R, Terburg D, Morgan B, Stein DJ, van Honk J, de Gelder B (2016): The role of the basolateral amygdala in the perception of faces in natural contexts. Philos Trans R Soc B Biol Sci 371:37–48.

3. Hibar DP, Stein JL, Renteria ME, Arias-Vasquez A, Desrivières S, Jahanshad N, *et al.* (2015): Common genetic variants influence human subcortical brain structures. Nature 520:224–229.
4. Satizabal CL, Adams HHH, Hibar DP, White CC, Knol MJ, Stein JL, *et al.* (2019): Genetic architecture of subcortical brain structures in 38, 851 individuals. Nat Genet 51:1624–1636.
5. Janak PH, Tye KM (2015): From circuits to behaviour in the amygdala. Nature 517:284–292.
6. Jovanovic T, Norrholm SD, Blanding NQ, Davis M, Duncan E, Bradley B, Ressler KJ (2010): Impaired fear inhibition is a biomarker of PTSD but not depression. Depress Anxiety 27:244–251.
7. Cádiz-Moretti B, Martínez-García F, Lanuza E (2013): Neural substrate to associate odorants and pheromones: Convergence of projections from the main and accessory olfactory bulbs in mice. In: East M, Dehnhard M, editors. Chemical Signals in Vertebrates, vol. 12. New York: Springer, 3–16.
8. Bzdok D, Laird AR, Zilles K, Fox PT, Eickhoff SB (2013): An investigation of the structural, connectional, and functional subspecialization in the human amygdala. Hum Brain Mapp 34:3247–3266.
9. Saygin ZM, Kliemann D, Iglesias JE, van der Kouwe AJW, Boyd E, Reuter M, *et al.* (2017): High-resolution magnetic resonance imaging reveals nuclei of the human amygdala: Manual segmentation to automatic atlas. Neuroimage 155:370–382.
10. Okada N, Fukunaga M, Yamashita F, Koshiyama D, Yamamori H, Ohi K, *et al.* (2016): Abnormal asymmetries in subcortical brain volume in schizophrenia. Mol Psychiatry 21:1460–1466.
11. Hibar DP, Westlye LT, Van Erp TGM, Rasmussen J, Leonardo CD, Faskowitz J, *et al.* (2016): Subcortical volumetric abnormalities in bipolar disorder. Mol Psychiatry 21:1710–1716.
12. Morey RA, Gold AL, LaBar KS, Beall SK, Brown VM, Haswell CC, *et al.* (2012): Amygdala volume changes in posttraumatic stress disorder in a large case-controlled veterans group. Arch Gen Psychiatry 69:1169–1178.
13. Chen LW, Sun D, Davis SL, Haswell CC, Dennis EL, Swanson CA, *et al.* (2018): Smaller hippocampal CA1 subfield volume in posttraumatic stress disorder. Depress Anxiety 35:1018–1029.
14. Fujishiro H, Tsuboi Y, Lin WL, Uchikado H, Dickson DW (2008): Co-localization of tau and α-synuclein in the olfactory bulb in Alzheimer's disease with amygdala Lewy bodies. Acta Neuropathol 116:17–24.
15. Barth C, Nerland S, de Lange AG, Wortinger LA, Hilland E, Andreassen OA, *et al.* (2021): In vivo amygdala nuclei volumes in schizophrenia and bipolar disorders. Schizophr Bull 47:1431–1441.
16. van der Meer D, Rokicki J, Kaufmann T, Córdova-Palomera A, Moberget T, Alnæs D, *et al.* (2020): Brain scans from 21,297 individuals reveal the genetic architecture of hippocampal subfield volumes. Mol Psychiatry 25:3053–3065.
17. Elvsåshagen T, Bahrami S, van der Meer D, Agartz I, Alnæs D, Barch DM, *et al.* (2020): The genetic architecture of human brainstem structures and their involvement in common brain disorders. Nat Commun 11:4016.
18. Elvsåshagen T, Shadrin A, Frei O, van der Meer D, Bahrami S, Kumar VJ, *et al.* (2021): The genetic architecture of the human thalamus and its overlap with ten common brain disorders. Nat Commun 12:2909.
19. Miller KL, Alfaro-Almagro F, Bangerter NK, Thomas DL, Yacoub E, Xu J, *et al.* (2016): Multimodal population brain imaging in the UK Biobank prospective epidemiological study. Nat Neurosci 19:1523–1536.
20. Bycroft C, Freeman C, Petkova D, Band G, Elliott LT, Sharp K, *et al.* (2018): The UK biobank resource with deep phenotyping and genomic data. Nature 562:203–209.
21. Quattrini G, Pievani M, Jovicich J, Aiello M, Bargalló N, Barkhof F, *et al.* (2020): Amygdalar nuclei and hippocampal subfields on MRI: Test–retest reliability of automated volumetry across different MRI sites and vendors. Neuroimage 218:116932.
22. Rosen AFG, Roalf DR, Ruparel K, Blake J, Seelaus K, Villa LP, *et al.* (2018): Quantitative assessment of structural image quality. Neuroimage 169:407–418.
23. Reich D, Price AL, Patterson N (2008): Principal component analysis of genetic data. Nat Genet 40:491–492.
24. Chang CC, Chow CC, Tellier LCAM, Vattikuti S, Purcell SM, Lee JJ (2015): Second-generation PLINK: Rising to the challenge of larger and richer datasets. GigaScience 4:7.
25. Watanabe K, Taskesen E, Van Bochoven A, Posthuma D (2017): Functional mapping and annotation of genetic associations with FUMA. Nat Commun 8:1826.
26. Yang J, Lee SH, Goddard ME, Visscher PM (2011): GCTA: A tool for genome-wide complex trait analysis. Am J Hum Genet 88:76–82.
27. Zaitlen N, Kraft P, Patterson N, Pasaniuc B, Bhatia G, Pollack S, Price AL (2013): Using extended genealogy to estimate components of heritability for 23 quantitative and dichotomous traits. PLoS Genet 9: e1003520.
28. Bulik-Sullivan BK, Loh PR, Finucane HK, Ripke S, Yang J, Schizophrenia Working Group of the Psychiatric Genomics Consortium, *et al.* (2015): LD score regression distinguishes confounding from polygenicity in genome-wide association studies. Nat Genet 47:291–295.
29. Bulik-Sullivan B, Finucane HK, Anttila V, Gusev A, Day FR, Loh PR, *et al.* (2015): An atlas of genetic correlations across human diseases and traits. Nat Genet 47:1236–1241.
30. Frei O, Holland D, Smeland OB, Shadrin AA, Fan CC, Maeland S, *et al.* (2019): Bivariate causal mixture model quantifies polygenic overlap between complex traits beyond genetic correlation. Nat Commun 10:2417.
31. Andreassen OA, Djurovic S, Thompson WK, Schork AJ, Kendler KS, O'Donovan MC, *et al.* (2013): Improved detection of common variants associated with schizophrenia by leveraging pleiotropy with cardiovascular-disease risk factors. Am J Hum Genet 92:197–209.
32. Walters RK, Polimanti R, Johnson EC, McClintick JN, Adams MJ, Adkins AE, *et al.* (2018): Transancestral GWAS of alcohol dependence reveals common genetic underpinnings with psychiatric disorders. Nat Neurosci 21:1656–1669.
33. Lambert JC, Ibrahim-Verbaas CA, Harold D, Naj AC, Sims R, Bellenguez C, *et al.* (2013): Meta-analysis of 74,046 individuals identifies 11 new susceptibility loci for Alzheimer's disease. Nat Genet 45:1452–1458.
34. Autism Spectrum Disorders Working Group of The Psychiatric Genomics Consortium (2017): Meta-analysis of GWAS of over 16,000 individuals with autism spectrum disorder highlights a novel locus at 10q24.32 and a significant overlap with schizophrenia. Mol Autism 8:21.
35. Otowa T, Hek K, Lee M, Byrne EM, Mirza SS, Nivard MG, *et al.* (2016): Meta-analysis of genome-wide association studies of anxiety disorders [published correction appears in Mol Psychiatry 2016; 21:1485. Mol Psychiatry 21:1391–1399.
36. Stahl EA, Breen G, Forstner AJ, McQuillin A, Ripke S, Trubetskoy V, *et al.* (2019): Genome-wide association study identifies 30 loci associated with bipolar disorder. Nat Genet 51:793–803.
37. Nalls MA, Pankratz N, Lill CM, Do CB, Hernandez DG, Saad M, *et al.* (2014): Large-scale meta-analysis of genome-wide association data identifies six new risk loci for Parkinson's disease. Nat Genet 46:989–993.
38. Schizophrenia Working Group of the Psychiatric Genomics Consortium (2014): Biological insights from 108 schizophrenia-associated genetic loci. Nature 511:421–427.
39. Benarroch EE (2015): The amygdala: Functional organization and involvement in neurologic disorders. Neurology 84:313–324.
40. Holland D, Frei O, Desikan R, Fan CC, Shadrin AA, Smeland OB, *et al.* (2020): Beyond SNP heritability: Polygenicity and discoverability of phenotypes estimated with a univariate Gaussian mixture model. PLoS Genet 16:e1008612.
41. Krishna Kumar S, Feldman MW, Rehkopf DH, Tuljapurkar S (2016): Limitations of GCTA as a solution to the missing heritability problem. Proc Natl Acad Sci USA 113:E61–E70.
42. Ward JH (1963): Hierarchical grouping to optimize an objective function. J Am Stat Assoc 58:236–244.
43. Cirulli ET, Kasperaviciūte D, Attix DK, Need AC, Ge D, Gibson G, Goldstein DB (2010): Common genetic variation and performance on standardized cognitive tests. Eur J Hum Genet 18:815–820.

44. Smith EN, Bloss CS, Badner JA, Barrett T, Belmonte PL, Berrettini W, *et al.* (2009): Genome-wide association study of bipolar disorder in European American and African American individuals. Mol Psychiatry 14:755–763.
45. Lin DY, Zeng D (2010): On the relative efficiency of using summary statistics versus individual-level data in meta-analysis. Biometrika 97:321–332.
46. Zenebe-Gete S, Salowe R, O'Brien JM (2021): Benefits of cohort studies in a consortia-dominated landscape. Front Genet 12: 801653.
47. Quansah E, McGregor NW (2018): Towards diversity in genomics: The emergence of neurogenomics in Africa? Genomics 110:1–9.
48. Cook JP, Morris AP (2016): Multi-ethnic genome-wide association study identifies novel locus for type 2 diabetes susceptibility. Eur J Hum Genet 24:1175–1180.
49. Fry A, Littlejohns TJ, Sudlow C, Doherty N, Adamska L, Sprosen T, *et al.* (2017): Comparison of sociodemographic and health-related characteristics of UK Biobank participants with those of the general population. Am J Epidemiol 186:1026–1034.
50. Bennett FC, Molofsky AV (2019): The immune system and psychiatric disease: A basic science perspective. Clin Exp Immunol 197:294–307.
51. Sekar A, Bialas AR, De Rivera H, Davis A, Hammond TR, Kamitaki N, *et al.* (2016): Schizophrenia risk from complex variation of complement component 4. Nature 530:177–183.
52. Onore C, Careaga M, Ashwood P (2012): The role of immune dysfunction in the pathophysiology of autism. Brain Behav Immun 26:383–392.
53. Passos IC, Vasconcelos-Moreno MP, Costa LG, Kunz M, Brietzke E, Quevedo J, *et al.* (2015): Inflammatory markers in post-traumatic stress disorder: A systematic review, meta-analysis, and meta-regression. Lancet Psychiatry 2:1002–1012.
54. Zorrilla EP, Luborsky L, McKay JR, Rosenthal R, Houldin A, Tax A, *et al.* (2001): The relationship of depression and stressors to immunological assays: A meta-analytic review. Brain Behav Immun 15:199–226.
55. Knuesel I, Chicha L, Britschgi M, Schobel SA, Bodmer M, Hellings JA, *et al.* (2014): Maternal immune activation and abnormal brain development across CNS disorders. Nat Rev Neurol 10:643–660.
56. Krabbe G, Minami SS, Etchegaray JI, Taneja P, Djukic B, Davalos D, *et al.* (2017): Microglial NFκB-TNFα hyperactivation induces obsessive–compulsive behavior in mouse models of progranulin-deficient Frontotemporal dementia. Proc Natl Acad Sci USA 114:5029–5034.
57. Zhan Y, Paolicelli RC, Sforazzini F, Weinhard L, Bolasco G, Pagani F, *et al.* (2014): Deficient neuron-microglia signaling results in impaired functional brain connectivity and social behavior. Nat Neurosci 17:400–406.
58. Alexander B, Georgiou-Karistianis N, Beare R, Ahveninen LM, Lorenzetti V, Stout JC, Glikmann-Johnston Y (2020): Accuracy of automated amygdala MRI segmentation approaches in Huntington's disease in the IMAGE-HD cohort. Hum Brain Mapp 41:1875–1888.
59. Thompson CL, Pathak SD, Jeromin A, Ng LL, MacPherson CR, Mortrud MT, *et al.* (2008): Genomic anatomy of the hippocampus. Neuron 60:1010–1021.
60. Fan CC, Smeland OB, Schork AJ, Chen CH, Holland D, Lo MT, *et al.* (2018): Beyond heritability: Improving discoverability in imaging genetics. Hum Mol Genet 27:R22–R28.